ARTICLES

APP binds DR6 to trigger axon pruning and neuron death via distinct caspases

Anatoly Nikolaev[1], Todd McLaughlin[2], Dennis D. M. O'Leary[2] & Marc Tessier-Lavigne[1]

Naturally occurring axonal pruning and neuronal cell death help to sculpt neuronal connections during development, but their mechanistic basis remains poorly understood. Here we report that β-amyloid precursor protein (APP) and death receptor 6 (DR6, also known as TNFRSF21) activate a widespread caspase-dependent self-destruction program. DR6 is broadly expressed by developing neurons, and is required for normal cell body death and axonal pruning both *in vivo* and after trophic-factor deprivation *in vitro*. Unlike neuronal cell body apoptosis, which requires caspase 3, we show that axonal degeneration requires caspase 6, which is activated in a punctate pattern that parallels the pattern of axonal fragmentation. DR6 is activated locally by an inactive surface ligand(s) that is released in an active form after trophic-factor deprivation, and we identify APP as a DR6 ligand. Trophic-factor deprivation triggers the shedding of surface APP in a β-secretase (BACE)-dependent manner. Loss- and gain-of-function studies support a model in which a cleaved amino-terminal fragment of APP (N-APP) binds DR6 and triggers degeneration. Genetic support is provided by a common neuromuscular junction phenotype in mutant mice. Our results indicate that APP and DR6 are components of a neuronal self-destruction pathway, and suggest that an extracellular fragment of APP, acting via DR6 and caspase 6, contributes to Alzheimer's disease.

The initial formative phase of nervous system development, involving the generation of neurons and extension of axons, is followed by a regressive phase in which inappropriate axonal branches are pruned to refine connections, and many neurons are culled to match the numbers of neurons and target cells[1–3]. The loss of neurons and branches also occurs in the adult after injury, and underlies the pathophysiology of many neurodegenerative diseases[1,4].

Our understanding of regressive events in development remains fragmentary. Degeneration can result 'passively' from the loss of support from trophic factors such as nerve growth factor (NGF)[1–3]. There is also evidence for 'active' mechanisms in which extrinsic signals trigger degeneration by means of pro-apoptotic receptors, including some members of the tumour necrosis factor (TNF) receptor superfamily such as p75NTR (also known as NGFR), Fas and TNFRSF1A (previously known as TNFR1) (Fig. 1a)[5]. However, the full complement of degeneration triggers remains incompletely understood.

Our understanding of the intracellular mechanisms of neuronal dismantling is also incomplete. It is well documented that developmental neuronal cell body degeneration requires the apoptotic

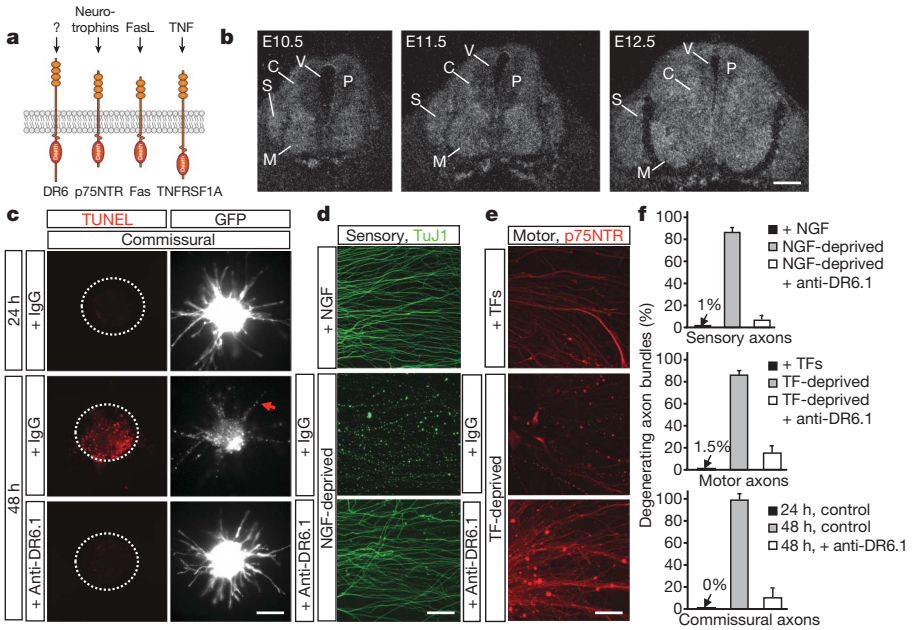

Figure 1 | DR6 regulates degeneration of several neuronal classes. **a**, Diagram of several TNF receptor superfamily members possessing death domains. **b**, *DR6* mRNA is expressed by differentiating spinal neurons (including motor (M) and commissural (C)), and by sensory (S) neurons in DRG at E10.5–E12.5. Expression is low in neuronal progenitors (P) in the ventricular zone (V). **c**–**f**, Anti-DR6.1 (50 μg ml^{-1}) reduces degeneration *in vitro*. **c**, Anti-DR6.1 inhibits commissural axon degeneration (visualized with green fluorescent protein (GFP), right) and cell body death (TUNEL labelling, left; dots indicate explants) seen after 48 h in dorsal spinal cord cultures. Red arrow indicates degenerating axon. **d**, **e**, Effect on degeneration of sensory (**d**) or motor (**e**) axons triggered by trophic deprivation. TFs, trophic factors (BDNF and NT3). Axons were visualized by immunostaining for tubulin (TuJ1; sensory) or p75NTR (motor). **f**, The percentage of degenerating axon bundles in **c**–**e** (mean and s.e.m., $n = 3$ replicates). Scale bars, 110 μm (**b**, **c**) and 50 μm (**d**, **e**).

[1]Division of Research, Genentech, Inc., 1 DNA Way, South San Francisco, California 94080, USA. [2]Molecular Neurobiology Laboratory, The Salk Institute, 10010 North Torrey Pines Road, La Jolla, California 92037, USA.

effectors BAX and caspase 3 (refs 6–8); pruning of a particular dendrite in *Drosophila* is also caspase-dependent[9,10]. Developmental axonal degeneration similarly has many hallmarks of apoptosis—including blebbing, fragmentation, and phagocytic clearing of debris by neighbouring cells[2,4]. However, it has been argued that axonal degeneration is caspase-independent, because caspase 3 inhibitors block cell body but not axonal degeneration[8] (reflecting higher activation of caspase 3 in cell bodies compared to axons[11]), and because genetic manipulations to inhibit apoptosis did not block axonal degeneration in some models[12,13]. These results indicated the existence of a caspase-independent program of axonal degeneration[1,2,4], but its molecular nature has remained elusive.

While studying the expression of all TNF receptor superfamily members[14], we found that DR6—one of eight members possessing a cytoplasmic death domain (Fig. 1a)—is widely expressed by neurons as they differentiate and enter a pro-apoptotic state. DR6 is an orphan receptor[15]. In transfected cells, it triggers cell death in a Jun N-terminal kinase-dependent manner[16]. *In vivo*, it regulates lymphocyte development[17,18], but its involvement in neural development is unknown.

Here we show that DR6 links passive and active degeneration mechanisms. After trophic deprivation, DR6 triggers neuronal cell body and axon degeneration. Because DR6 signals via BAX and caspase 3 in cell bodies, we revisited the involvement of caspases in axonal degeneration, and found that axonal degeneration indeed requires both BAX and a distinct effector, caspase 6. Our results also indicated that DR6 is activated by a prodegenerative ligand(s) that is surface-tethered but released in an active form after trophic deprivation. In searching for candidate ligands with these properties, we considered APP, a transmembrane protein that undergoes regulated shedding and is causally implicated in Alzheimer's disease[19–22], because we had previously found it to be highly expressed by developing neurons and especially axons (see later). Because Alzheimer's disease is marked by neuronal and axonal degeneration, we had long wondered whether APP participates in developmental degeneration. We show that an extracellular fragment of APP is indeed a ligand for DR6—as is a fragment of its close relative APLP2—that triggers degeneration of cell bodies via caspase 3 and axons via caspase 6, and we propose that this developmental mechanism is hijacked in Alzheimer's disease.

DR6 regulates neuronal death

To explore the involvement of the TNF receptor superfamily in neural development, we screened its 28 members by *in situ* hybridization in midgestation mouse embryos. We came to focus on DR6 (Fig. 1a), because its messenger RNA is expressed at low levels in proliferating progenitors in the spinal cord, but is highly expressed by differentiating neurons within the spinal cord and adjacent dorsal root ganglia (DRG) (Fig. 1b).

Because *DR6*-expressing neurons are becoming dependent for survival on trophic support at these stages, we examined whether DR6 regulates neuronal death after trophic-factor deprivation *in vitro*, focusing on three sets of spinal neurons: commissural, motor and sensory (Supplementary Fig. 1a). Initially, we found that short interfering RNA (siRNA) knockdown of *DR6* protected commissural neurons from degeneration (Supplementary Fig. 2). This prompted us to screen monoclonal antibodies to DR6 for their ability to mimic this protection; we selected antibody 3F4 (anti-DR6.1). When embryonic day (E)13.5 rat dorsal spinal cord explants are cultured for 24 h, commissural cell bodies and axons are healthy, but they degenerate if cultured for 24 h longer [23]; anti-DR6.1 inhibited this degeneration (Fig. 1c, f), mimicking *DR6* knockdown. Anti-DR6.1 also protected sensory neurons from E12.5 mouse DRGs cultured for 48 h with NGF, and motor neurons from E12.5 mouse ventral spinal cord explants cultured for 24 h with brain-derived neurotrophic factor (BDNF) and neurotrophin 3 (NTF3, also known as NT3): when these cultures were deprived of trophic factor and cultured for 24 h longer, they showed massive cell death and axonal degeneration, which were largely inhibited by anti-DR6.1 (Fig. 1d–f and Supplementary Fig. 1b). Similar protection was observed when DRGs or ventral explants from a *DR6* null mutant[17] were deprived in the absence of anti-DR6.1 (Supplementary Fig. 4b and data not shown), confirming that anti-DR6.1 is function-blocking. DR6 inhibition (by antibody, siRNA or genetic deletion) caused a delay rather than a complete block, because more degeneration was observed in each case 24–48 h later (Fig. 2b, Supplementary Fig. 4b and data not shown). Consistent with a delay, there was a higher motor-neuron number at E14.5 in the *DR6* mutant, but this returned to the wild-type level by E18 (Supplementary Fig. 3), after the cell death period. Thus, antagonizing DR6 delays the death of several neuronal populations *in vitro* and *in vivo*.

DR6 regulates axonal pruning

DR6 protein is expressed not just by cell bodies (data not shown) but also by axons (Supplementary Fig. 4a). Protection of axons by DR6

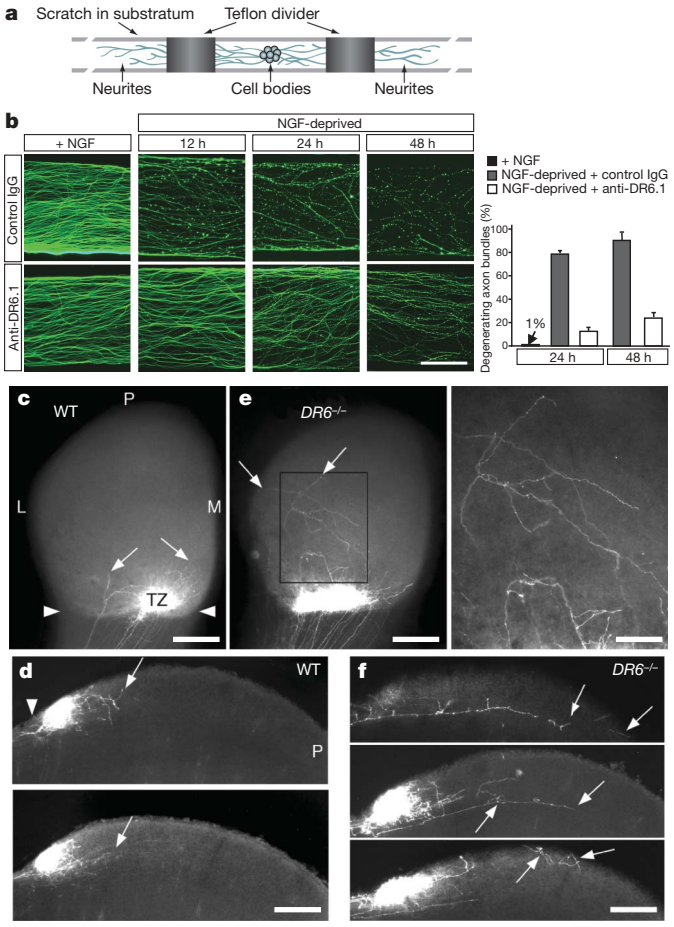

Figure 2 | DR6 regulates axon pruning *in vitro* and *in vivo*. **a**, Diagram of Campenot chamber (adapted from ref. 24). **b**, Images show the local degeneration of sensory axons (TuJ1 immunostain) in Campenot chambers after NGF deprivation from the axonal compartment (top) was delayed by anti-DR6.1 (50 μg ml^{-1}) added at the time of deprivation (bottom). The graph shows the percentage of degenerating bundles at 24 and 48 h (mean and s.e.m., $n = 3$ replicates). **c**–**f**, Compromised pruning of retinal axons in *DR6*$^{-/-}$ mice. Dorsal view of (**c**, **e**), and vibratome sections through (**d**, **f**), the superior colliculus of wild-type (WT; **c**, **d**) or *DR6*$^{-/-}$ (**e**, **f**) mice at P6. In wild-type mice (**c**, **d**), DiI-labelled temporal RGC axons form a dense termination zone (TZ) in anterior superior colliculus (arrowheads denote the anterior border). Few are outside the immediate termination zone area (arrows). In *DR6*$^{-/-}$ mice (**e**, **f**), temporal RGC axons and arbors are present in areas far from the termination zone (inset, magnified in **e**, right) and well posterior to it (arrows). L, lateral; M, medial; P, posterior. Scale bars, 100 μm (**b**), 400 μm (**c**, **e**, left), 170 μm (**e**, right) and 250 μm (**d**, **f**).

inhibition might therefore reflect a direct role for DR6 in axons. To explore this, we used compartmented ('Campenot') chambers[24] (Fig. 2a). Sensory neurons are placed in a central chamber containing NGF; their axons grow under a partition into NGF-containing side-chambers. Fluid exchange between the chambers is limited, so NGF deprivation in a side-chamber elicits local axon degeneration while sparing cell bodies[24]. Locally deprived axons degenerate in a stereotypical manner with initial signs by 6 h and extensive degeneration by 12–24 h, but when anti-DR6.1 was added to the deprived side-chamber, degeneration was blocked at 24 h and still largely impaired at 48 h (Fig. 2b). A similar delay was observed when axons of neurons from *DR6* knockout mice were locally deprived, but in the absence of anti-DR6.1 (Supplementary Fig. 4b, c). Thus, DR6 function is required in axons for degeneration.

To determine whether DR6 functions in axonal pruning *in vivo*, we studied the well-characterized retino-collicular projection, which develops from an initially exuberant projection of retinal ganglion cell (RGC) axons to a focused termination zone in the superior colliculus. All temporal RGC axons initially extend into posterior superior colliculus, well past their future termination zone in anterior superior colliculus (Supplementary Fig. 5a). This diffuse projection is then refined by selective degeneration of inappropriate axon segments[2], such that by postnatal day (P)6 in wild-type mice few axon segments persist in areas well beyond the termination zone, as revealed by focal injection of the lipophilic dye DiI into temporal retina (Fig. 2c, d and Supplementary Fig. 5a, b). In contrast, in P6 *DR6* mutant mice, many more RGC axons and arbors are present in areas far from the termination zone (Fig. 2e, f and Supplementary Fig. 5c, d): we found an 83% increase in axon-positive domains more than 400 μm from the termination zone (Supplementary Fig. 5f) in $DR6^{-/-}$ ($n = 7$) compared to wild-type mice ($n = 7$; $P < 0.05$, Student's *t*-test). The defect at P6 represents a delay in pruning, not a complete block, as assessed by examining labelled axons at P4, P5, P6 and P9: at each age, the mutant has more extraneous axons than the wild-type, and fewer are observed in both wild-type and mutant at each age compared to earlier time points, but by P9 the mutant and wild-type projections are indistinguishable (data not shown). Thus, blocking DR6 function delays pruning of sensory axons *in vitro* and retinocollicular axons *in vivo*.

Caspase 6 regulates axonal degeneration

Because DR6 regulates both cell body apoptosis and axonal degeneration, we revisited whether an apoptotic pathway is also involved in axons. In support, we found that BAX, an effector in the intrinsic apoptotic pathway, is required in axons, because local sensory axon degeneration in Campenot chambers was blocked by the genetic deletion of *Bax* (Fig. 3a) or by local addition of a BAX inhibitor (for example, Supplementary Fig. 10b). Consistent with evidence that caspase 3 mediates cell body but not axon degeneration[8,11], we found that procaspase 3 is highly enriched in cell bodies, and that zDEVD-fmk, an inhibitor of effector caspases 3 and 7, blocked cell body but not axon degeneration (Fig. 3b, c and Supplementary Fig. 6a–c). There is, however, a third effector caspase, caspase 6. We found that procaspase 6 is expressed in both cell bodies and axons, and that the caspase 6 inhibitor zVEID-fmk blocked degeneration of sensory, motor and commissural axons (Fig. 3b, c and Supplementary Fig. 6a–c), suggesting that caspase 6 regulates axonal degeneration. We verified these results using RNA interference in sensory and commissural neurons: *Casp3* knockdown protected cell bodies significantly but had only a minor protective effect on axons, whereas *Casp6* knockdown protected axons significantly with only minor effect on cell bodies (Fig. 3d, e). Thus, distinct caspases mediate cell body and axon degeneration.

To visualize caspase activation, we first used the fluorescent reporters FAM-DEVD-fmk (for caspase 3 and 7) and FAM-VEID-fmk (for caspase 6), which bind covalently to activated target caspases. In NGF-deprived sensory neurons, the caspase 3/7 reporter labelled cell bodies but not axons, consistent with a previous study[11]; in contrast, caspase 6 reporter labelling was observed in both cell bodies and axons, and axonal labelling occurred in regularly spaced 'puncta', giving a beads-on-a-string appearance (Supplementary Fig. 6f). To control for reporter specificity, we used a selective antibody to cleaved caspase 6 and observed a similar punctate pattern in axons (Fig. 3f, g), whereas antibodies to cleaved caspase 3 only label cell bodies[11]. Caspase 6 activation was confirmed biochemically (Supplementary Fig. 6e). Interestingly, caspase 6 activation appeared at sites of microtubule fragmentation (assessed by the loss of tubulin immunoreactivity) (Fig. 3f, g), suggesting that caspase 6 activation drives microtubule destabilization. Punctate caspase 6 activation was markedly reduced by anti-DR6.1 (Fig. 3f) and abolished in $Bax^{-/-}$ neurons (not shown), suggesting that caspase 6 acts downstream of BAX in the pathway triggered by DR6. However, the possibility of feedback loops in apoptotic pathways makes this interpretation tentative.

Regulated shedding of a DR6 ligand(s)

As DR6 is a receptor-like protein, we addressed whether it is activated by a ligand(s). If so, the DR6 ectodomain might be capable of binding the ligand(s) and blocking its action (Fig. 4a). Consistent with this, the DR6 ectodomain fused to human Fc (DR6–Fc) mimicked anti-DR6.1 in delaying degeneration (Fig. 4a–c and Supplementary Figs 7a and 13). To search for DR6 binding sites on axons and in conditioned medium, we used the DR6 ectodomain fused to alkaline phosphatase (DR6–AP). Purple alkaline phosphatase reaction product was observed on sensory and motor axons cultured with trophic factors when they were pre-incubated with DR6–AP but not with alkaline phosphatase alone, but binding was markedly reduced after trophic deprivation (Supplementary Fig. 7b, c). To control for the loss of axonal membrane, we blocked degeneration using a BAX inhibitor (data not shown) or using neurons from $Bax^{-/-}$ mice (Fig. 4d) and observed an even greater reduction in DR6–AP binding (residual binding seen without BAX inhibition might reflect nonspecific binding to degenerating axons). To determine whether DR6-binding sites were shed, we collected medium conditioned by sensory axons (in Campenot chambers) or motor neurons (in explant culture) (a BAX inhibitor was added to prevent nonspecific release resulting from degeneration). Proteins were separated on non-reducing gels, blotted to nitrocellulose, and probed with DR6–AP. Little signal was seen in medium conditioned by either neuronal type in the presence of trophic factor. However, 48 h after trophic deprivation, DR6–AP bound a prominent band around ~35 kDa and a minor band around ~100 kDa in both cultures (Fig. 4e). Together, these results support a 'ligand activation' model in which a prodegenerative DR6 ligand(s) is present on the neuronal surface and inactive, but is shed into medium in an active form after trophic deprivation (Fig. 4f), allowing it to bind and activate DR6.

N-APP is a regulated DR6 ligand

Several properties of APP made it a candidate for a DR6 ligand: (1) it is highly expressed by developing spinal and sensory neurons and their axons (Fig. 4g), (2) its ectodomain can be shed in a regulated fashion[19,20], and (3) it is tied to degeneration through its links to Alzheimer's disease[19–22]. In an initial experiment, we found that DR6–AP bound APP expressed in COS-1 cells (Supplementary Fig. 8a). This prompted us to test whether the bands detected by DR6–AP in conditioned medium (Fig. 4e) represent APP ectodomain fragments. APP is cleaved by α- or β-secretases (including, in neurons, BACE1; ref. 25) at distinct sites in its juxtamembrane region (Fig. 4h) to release ~100-kDa ectodomain fragments termed sAPPα or sAPPβ, respectively[19,20]. We probed conditioned medium with a polyclonal antibody to the APP N terminus (anti-N-APP(poly), which also binds the APP relative APLP2; see later) and an antibody selective for the carboxy-terminal epitope of sAPPβ exposed by BACE cleavage (anti-sAPPβ) (Fig. 4h). Notably, anti-N-APP(poly) detected

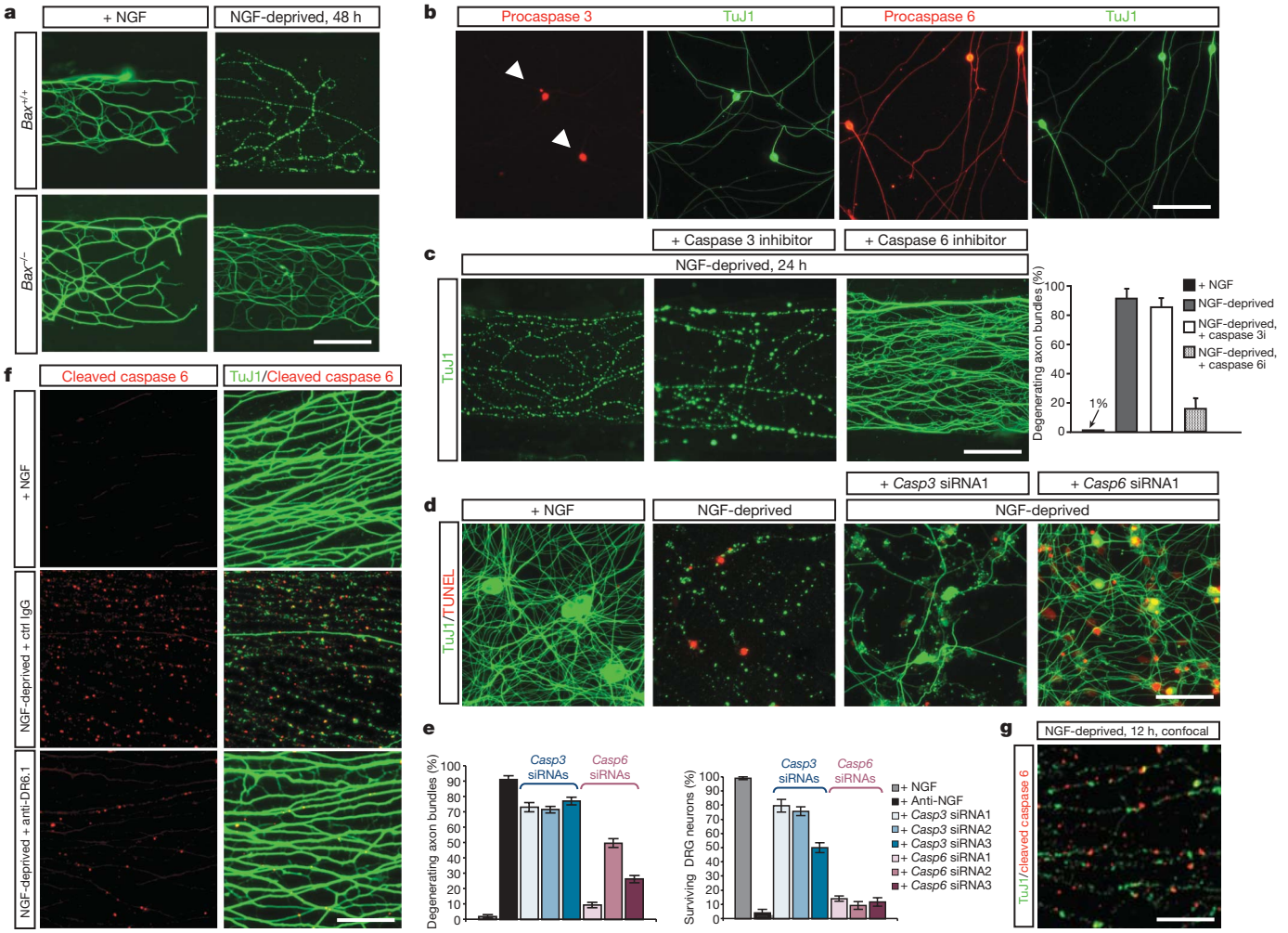

Figure 3 | BAX and caspase 6 regulate axonal degeneration. **a**, Local sensory axon degeneration (TuJ1 immunostain) 48 h after NGF deprivation in Campenot chambers was blocked in neurons from *Bax*$^{-/-}$ mice. **b**, Dissociated sensory neurons double-labelled for procaspase 3 and TuJ1 (left), or procaspase 6 and TuJ1 (right). Caspase 3 is detected in cell bodies (arrowheads), whereas caspase 6 is seen in both cell bodies and axons. **c**, Local degeneration of sensory axons in Campenot chambers deprived of NGF for 24 h is inhibited by a caspase 6 inhibitor (zVEID-FMK; caspase 6i), but not by a caspase 3/7 inhibitor (zDEVD-FMK; caspase 3i). Quantification is shown to the right (mean and s.e.m., $n = 3$ replicates). **d**, In dissociated sensory neuron cultures deprived of NGF for 24 h, siRNA knockdown of *Casp3* primarily rescues cell body death (TUNEL label), whereas *Casp6* knockdown primarily rescues axonal degeneration. **e**, Quantification of data from **d**. Shown are the percentage of degenerating axon bundles (that is, still visible bundles that show breakdown) and the percentage of surviving neurons (that is, TUNEL$^-$, TuJ1$^+$) (mean ± s.e.m., $n = 3$ replicates). Note that surviving axons may have TUNEL$^+$ cell bodies. The extent of inhibition by individual siRNAs correlates with the degree of target knockdown (Supplementary Fig. 6d). **f**, Detection of caspase 6 activation in sensory axons with a cleaved caspase-6-specific antibody (left; TuJ1 double-label on right). Punctate activation of caspase 6 after NGF deprivation (16 h, middle panel) was reduced by anti-DR6.1 (bottom panel). **g**, Confocal section of a field from **f** shows that active caspase 6 puncta correspond to sites of tubulin loss (fraction non-overlapping: 82 ± 3.5%; mean ± s.e.m., $n = 8$ fields). Scale bars, 75 μm (**a**, **d**), 100 μm (**b**), 50 μm (**c**, **f**) and 25 μm (**g**).

similar bands to those detected by DR6–AP: a major band at ~35 kDa and a minor band at ~100 kDa, both highly enriched after trophic deprivation (Fig. 4i); anti-sAPPβ detected a minor ~100-kDa band and a major ~55-kDa band (Fig. 4i), also both enriched after trophic deprivation. These results indicate that trophic deprivation triggers BACE cleavage of APP to yield the ~100-kDa sAPPβ (detected by both antibodies), which undergoes a further cleavage(s) to yield a ~55-kDa C-terminal fragment (detected by anti-sAPPβ) and a ~35-kDa N-terminal fragment (detected by anti-N-APP(poly)) that we term N-APP. The site of additional cleavage(s) is unknown, but on the basis of fragment sizes it is expected to be around the junction between the APP 'acidic' and 'E2' domains (amino acid 286); indeed, recombinant APP(1–286) ran at ~35 kDa and was detected with anti-N-APP(poly) (Fig. 4j), similar to N-APP.

Supporting cleavage of APP by BACE, we found that APP expression on the surface of cultured sensory and motor axons, as assessed with anti-N-APP(poly) and with antibody 4G8 to the APP juxtamembrane region (Fig. 4h), is high in the presence of trophic factor but lost after trophic deprivation; the surface loss was blocked by three structurally divergent BACE inhibitors—OM99-2, BACE inhibitor IV, and the highly selective AZ29 (ref. 26) but not the α-secretase inhibitor TAPI (Fig. 4k, Supplementary Figs 9a–c and 10a, and data not shown). Interestingly, 4G8 partially inhibited surface loss (Supplementary Fig. 9d), presumably through the steric hindrance of BACE. Loss of surface APP occurred progressively and in 'patches', with little lost at 3 h, more at 6–12 h, and most lost by 24 h (Fig. 4k, Supplementary Fig. 10b and data not shown). Total APP visualized after permeabilization did not change detectably (Supplementary Fig. 10b). Surface loss was not affected by BAX or caspase 6 inhibitors, or in neurons from *Bax*$^{-/-}$ mice (Fig. 4k and Supplementary Figs 9c and 10c).

The marked similarly of bands detected by anti-N-APP(poly) and DR6–AP suggested that DR6 binds N-APP. Indeed, depletion of conditioned medium with anti-N-APP(poly) eliminated DR6–AP binding sites (Fig. 4i), and purified DR6–Fc bound to purified recombinant APP(1–286) in pull-down (Fig. 4j) and enzyme-linked

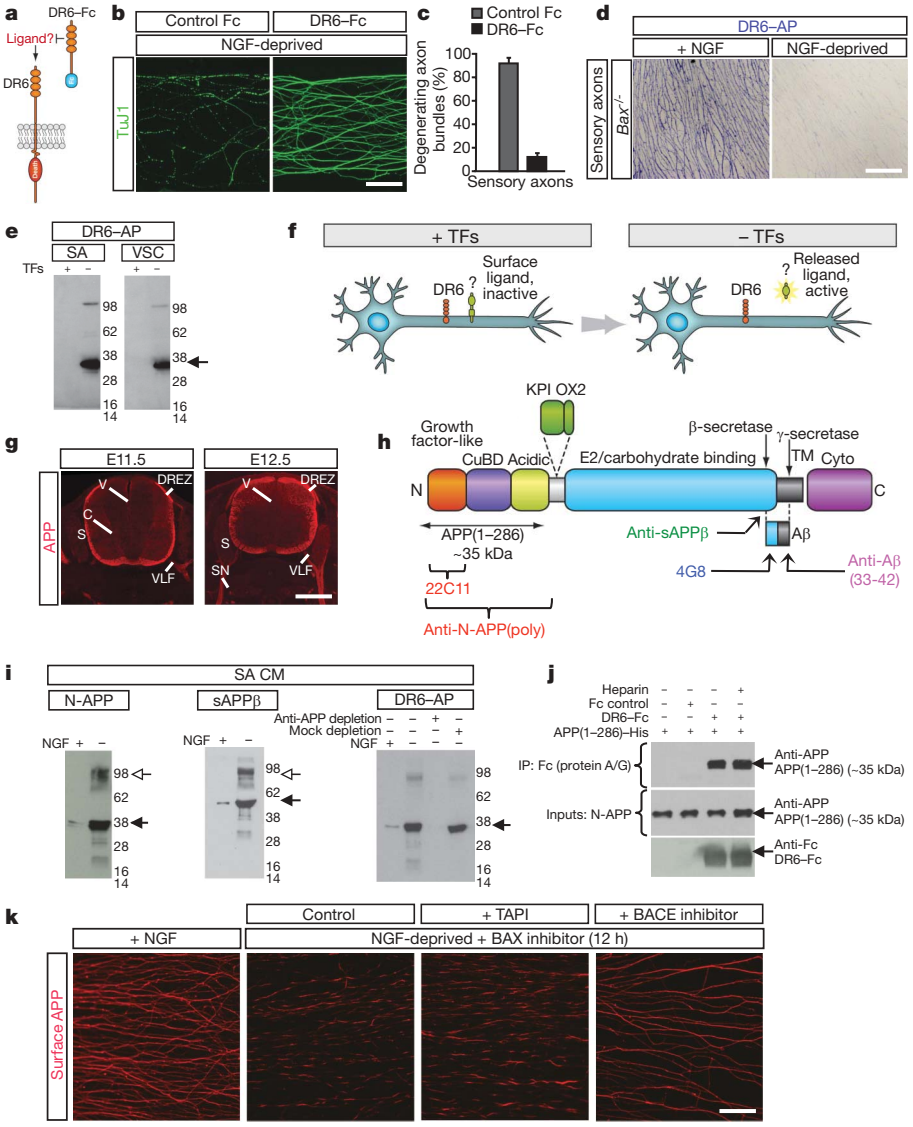

Figure 4 | The N terminus of APP is a regulated DR6 ligand. **a**, Diagram of the hypothesis: if DR6 is ligand-activated, then DR6–Fc might sequester ligand and inhibit degeneration. **b**, DR6–Fc inhibits local degeneration of sensory axons in Campenot chambers 24 h after NGF deprivation. **c**, Quantification of results in **b** (mean and s.e.m., $n = 3$ replicates). **d**, **e**, DR6-binding sites are lost from axons and released into medium after trophic deprivation. **d**, DR6–AP binding (purple) to $Bax^{-/-}$ sensory axons (left) is lost 24 h after NGF deprivation (right). **e**, Medium conditioned by sensory axons (SA) (in Campenot chambers) or ventral spinal cord explants (VSC), maintained with or deprived of trophic factors (TFs) for 24 h (sensory: NGF; motor: BDNF and NT3; BAX inhibitor present), was resolved under non-reducing conditions and probed with DR6–AP. The arrow indicates a major band at ~35 kDa. **f**, Results in **a**–**e** support a ligand activation model in which an inactive DR6 surface ligand is shed in an active form after tropic deprivation. **g**, APP immunostaining on sections of mouse embryos at indicated ages, showing neuronal and axonal expression. DREZ, dorsal root entry zone; S, sensory ganglia; SN, spinal nerve; V, ventricular zone; VLF, ventro-lateral funiculus. **h**, Domain structure of APP (short form, APP695), indicating β- and γ-secretase cleavage sites and antibody binding sites. KPI and OX2 denote alternatively spliced domains of the longer form. Adapted from ref. 20. Aβ, amyloid-β peptide; CuBD, copper binding domain; cyto, cytosolic domain; TM, transmembrane domain. **i**, DR6 binding sites in sensory axon conditioned medium (SA CM) include APP ectodomain fragments. Left, anti-N-APP(poly) detects bands at ~35 kDa (major; filled arrow) and ~100 kDa (minor; open arrow), enriched after trophic deprivation. Middle, anti-sAPPβ detects bands at ~55 kDa (major; filled arrow) and ~100 kDa (minor; open arrow). Right, immunodepletion using anti-N-APP(poly) depletes DR6–AP binding sites. Arrow indicates N-APP band at ~35 kDa. **j**, Direct interaction between purified APP(1–286) and DR6–Fc revealed by pull-down. The effect of heparin (10 μg ml^{-1}) was also examined. IP, immunoprecipitates. **k**, Loss of surface APP in patches from sensory axons 12 h after NGF deprivation is blocked by the BACE inhibitor OM99-2 (10 μM) but not by the α-secretase inhibitor TAPI (20 μM). Scale bars, 75 μm (**b**, **d**, **k**) and 500 μm (**g**).

immunosorbent assay (ELISA) (Supplementary Fig. 8c) assays. The interaction detected by ELISA is of high affinity (effector concentration for half-maximum response (EC_{50}) = ~4.6 nM). The interaction of DR6–AP with full-length APP expressed in COS cells was also of high affinity (half maximal saturation = ~1.3 nM) (Supplementary Fig. 8a, b). This binding was blocked by anti-N-APP(poly) (data not shown) and anti-DR6.1 (Supplementary Fig. 8a), consistent with APP being a functional DR6 ligand.

Antibodies 4G8 and anti-sAPPβ used earlier are highly specific for APP. However, like other antibodies to the N terminus of APP[27], anti-APP(poly) also binds the close APP relative APLP2 (data not shown). We found that a recombinant N-terminal fragment of APLP2 also binds DR6 (Supplementary Fig. 11a). Thus, APLP2 might contribute with APP to the bands detected on western by DR6–AP. Indeed, an antibody selective for the APLP2 N terminus detected a shed fragment in conditioned medium after trophic deprivation (Supplementary Fig. 11b). The relative contribution of APP and APLP2 fragments to DR6–AP binding sites remains to be determined.

To evaluate receptor specificity, we examined by pull-down the binding of APP(1–286) to ectodomains of the seven other

death-domain-containing members of the TNF receptor superfamily, and two orphan members. Only binding to p75NTR was observed (Supplementary Fig. 8d), suggesting that p75NTR might serve as an alternative route for APP effects in some settings; however, the affinity was considerably lower (EC_{50} = ~300 nM by ELISA; Supplementary Fig. 8e). Consistent with DR6 being the chief APP receptor in our systems, a fusion of APP(1–286) and alkaline phosphatase bound to sensory axons in culture, but the binding was significantly reduced by anti-DR6.1 or by using *DR6* knockout neurons (Supplementary Fig. 12a, b); residual binding may represent background or binding to another receptor(s), possibly p75NTR.

Necessity and sufficiency of N-APP

To test whether the N terminus of APP contributes to degeneration, we performed loss-of-function studies. Degeneration of sensory and commissural axons in response to trophic deprivation was inhibited by anti-N-APP(poly) (Fig. 5a, d), which also inhibited the death of sensory neuron cell bodies (Supplementary Fig. 13a, b), without affecting the loss of surface APP after trophic deprivation (Supplementary Fig. 13c). Antibody 22C11 (ref. 28) to the APP N terminus (Fig. 4h) also inhibited sensory axon degeneration (data not shown). Because both antibodies also bind APLP2 (ref. 27), we performed a more selective blockade using RNA interference. Knockdown of *App* in sensory neurons significantly impaired both axon degeneration and cell body death after trophic withdrawal (Fig. 5b). These results support the involvement of an N-terminal fragment of APP in degeneration. In further support, BACE inhibitors impaired degeneration of sensory axons and cell bodies (Fig. 5c and Supplementary Figs 13a, b and 14) and of commissural axons (Fig. 5d) after trophic deprivation. The selective BACE inhibitor AZ29 blocked degeneration at concentrations consistent with its cellular half-maximal inhibitory concentration (IC_{50}) of 470 nM[26] (Supplementary Fig. 14a).

Importantly, axonal degeneration block by BACE inhibitors could be reversed by adding purified APP(1–286) to sensory (Fig. 5c) and commissural (Fig. 5d) neurons, showing that the N terminus of APP is sufficient to trigger degeneration. This effect was largely blocked by anti-DR6.1 (Supplementary Fig. 14b), consistent with DR6 being the most important functional receptor in these cells. Block of sensory cell body degeneration by BACE inhibitors could similarly be reversed by the addition of APP(1–286), albeit at higher concentrations (Supplementary Fig. 13a, b). Together, these results support the model that shed N-APP activates DR6 to trigger degeneration. Degeneration of sensory axons caused by APP(1–286) in the presence of BACE inhibitor was blocked if NGF was present (50 ng ml^{-1}; Fig. 5c), indicating that trophic factors also inhibit signalling downstream of DR6.

Role of amyloid-β in physiological degeneration

BACE cleavage of APP is followed by γ-secretase cleavage, yielding amyloid-β peptides[19–22] (Figs 4h and 6c). Because amyloid-β peptides can be neurotoxic[21,22], we examined whether they contribute to degeneration. The synthetic amyloid-β peptide Aβ(1–42) triggered degeneration in our assays, and an antibody directed at amino acids 33–42 of amyloid-β (anti-Aβ(33–42); Fig. 4h) blocked this effect (Supplementary Fig. 9a, e), but did not block degeneration after trophic deprivation (Fig. 5e). Conversely, degeneration induced by synthetic Aβ(1–42) was not blocked by the genetic deletion of *DR6* (data not shown), indicating that amyloid-β operates by a mode of action distinct from the physiological degeneration mechanism studied here.

Antibody 4G8 used earlier, which binds amyloid-β residues 17–24 (Fig. 4h), also blocked the degenerative effect of Aβ(1–42) (Supplementary Fig. 9e), but unlike anti-Aβ(33–42) it partially inhibited degeneration after trophic deprivation (Fig. 5e). However, as mentioned, 4G8 also partially inhibits the loss of surface

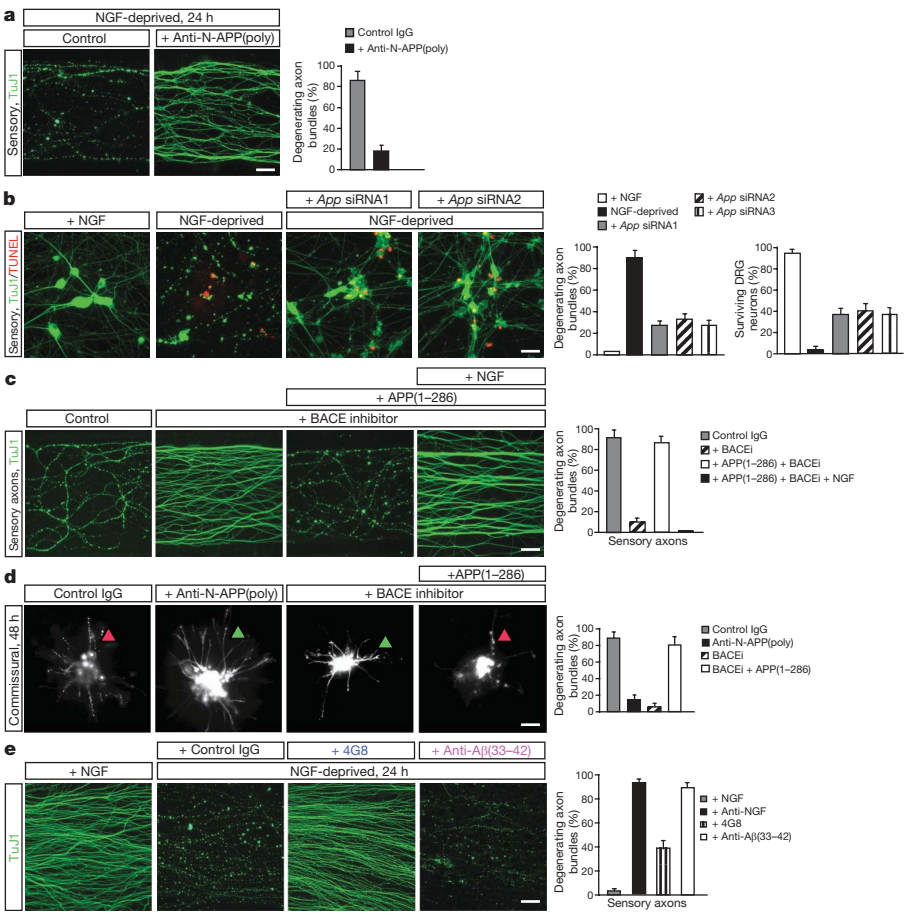

Figure 5 | The APP N terminus regulates degeneration. **a**, Local degeneration of sensory axons in Campenot chambers (NGF deprivation, 24 h) was blocked by anti-N-APP(poly) (20 μg ml^{-1}). Quantification is shown to the right for all panels (**a**–**e**). **b**, In dissociated sensory neurons, siRNA knockdown of *App* (Supplementary Fig. 13d) significantly reduces axon degeneration 24 h after trophic deprivation, and partially reduces cell body death. **c**, Local degeneration of sensory axons in Campenot chambers (NGF deprivation, 24 h) was inhibited by the local addition of BACE inhibitor (BACEi) OM99-2 (10 μM). Purified APP(1–286) added locally restored axonal degeneration, an effect inhibited by 50 ng ml^{-1} NGF (right). **d**, Degeneration of commissural neurons and axons at 48 h was inhibited by anti-N-APP(poly) (20 μg ml^{-1}) or BACE inhibitor OM99-2 (10 μM), but restored by APP(1–286). **e**, Effect of amyloid-β antibodies on sensory axon degeneration (NGF deprivation, 24 h). 4G8 partially inhibited, whereas anti-Aβ(33–42) did not. Scale bars 50 μm (**a**, **c**, **e**), 40 μm (**b**) and 200 μm (**d**). All data are mean and s.e.m. for $n = 3$ replicates.

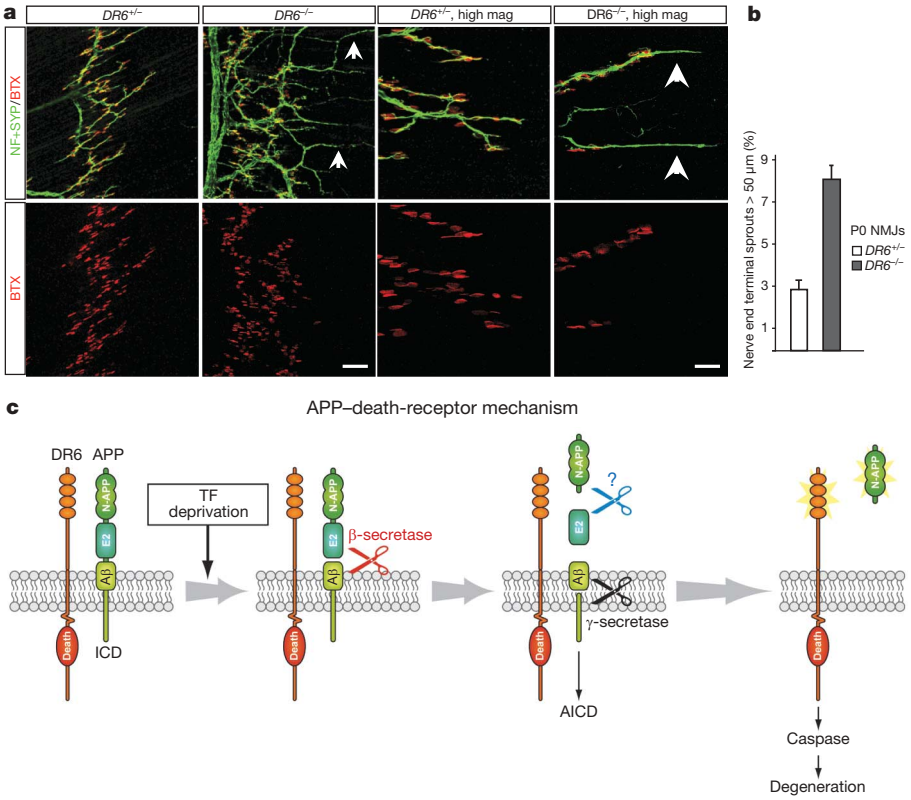

Figure 6 | APP and DR6 signalling: *in vivo* evidence, and model. **a**, In control ($DR6^{+/-}$) P0 diaphragm muscle, few axons (green, neurofilament (NF) and synaptophysin (SYP) stain) overshoot endplates (red, fluorescent α-bungarotoxin (BTX) stain), and those that do are short, but in *DR6* mutants more overshoot and many are long (arrowheads). Scale bar, 60 μm (left four panels) and 15 μm (right four panels). **b**, The number of axons overshooting by >50 μm (mean and s.e.m., $n = 3$ wild-type, 4 mutants); this underestimates the effect, because overshooting axons are longer in mutants. NMJ, neuromuscular junction. **c**, The APP–death-receptor mechanism is shown. Trophic factor (TF)-deprivation triggers the cleavage of surface APP by β-secretase, releasing sAPPβ, which is further cleaved by an unknown mechanism ('?') to release N-APP. This then binds DR6 to trigger degeneration through caspase 6 in axons and caspase 3 in cell bodies. Also illustrated is cleavage by γ-secretase to release amyloid-β (Aβ) and the APP intracellular domain (AICD).

APP. In contrast, the APP epitope bound by anti-Aβ(33–42) is buried in the cell membrane, so anti-Aβ(33–42) does not bind intact APP nor inhibit its surface loss (Supplementary Fig. 9a, b, d). Because anti-Aβ(33–42) does not protect, we attribute the partial protective effect of 4G8 to its ability to inhibit APP shedding, not its ability to block amyloid-β toxicity. Because 4G8 does not bind APLP2, its ability to protect also supports the sufficiency of APP in mediating degeneration.

Evidence for an APP–DR6 interaction *in vivo*

To seek evidence for an APP–DR6 interaction *in vivo*, we examined whether the *DR6* knockout exhibits any similar phenotype to those reported in the *App* knockout—or, given the potential for redundancy, in compound mutants of *App* with *Aplp2*. One phenotype observed at the neuromuscular junction in the $App^{-/-}$ $Aplp2^{-/-}$ double knockout is suggestive of a potential pruning defect. In wild-type animals, motor axons normally terminate at synaptic sites (Fig. 6a). In $App^{-/-}$ $Aplp2^{-/-}$ double knockouts, however, there is a highly penetrant presence of nerve terminals past endplates[29]. Notably, a similar phenotype was observed in the *DR6* mutant: rather than terminating at endplates, many terminals were present beyond, giving characteristic finger-like protrusions (Fig. 6a, b). It is not known whether this phenotype reflects a failure to retract or excessive sprouting. Nevertheless, the similarity of phenotypes supports the view that APP signals via DR6 in regulating axonal behaviour *in vivo*. In this system, APP and APLP2 appear redundant because the axonal phenotype is seen only in $App^{-/-}$ $Aplp2^{-/-}$ double mutants, not single mutants[29]. Whether they are non-redundant in other systems remains to be determined.

Discussion

Our results reveal a mechanism, the 'APP–death-receptor' mechanism (Fig. 6c), in which trophic deprivation leads to the cleavage of surface APP by β-secretase, followed by further cleavage of the released fragment by an as yet unidentified mechanism (probably near the junction of APP acidic and E2 domains). This then yields an N-terminal ~35-kDa fragment (N-APP) which binds DR6, triggering caspase activation and degeneration of both neuronal cell bodies (via caspase 3) and axons (via caspase 6). Whether the second cleavage is required for degeneration remains to be determined. Degeneration induced by added APP(1–286) was blocked when sufficient trophic factor was present, indicating that trophic factor not only prevents initiation of the APP cleavage cascade, but also blocks signalling downstream of DR6, providing a fail-safe mechanism to protect if DR6 is inappropriately activated in an otherwise healthy neuron.

DR6: an accelerator of self-destruction

In all settings examined, antagonizing DR6 resulted in a delay, rather than a complete block, in neuronal death and axonal pruning. DR6 is therefore best thought of as an accelerator of degeneration—neurons and axons activate it for swift self-destruction when they become atrophic, but without it they have other, slower, ways of achieving that end, perhaps involving other pro-apoptotic receptors[5] or intrinsic mechanisms. This function contrasts that of the DR6 relative p75NTR (which can mediate degeneration when overexpressed[11] or when activated by a neurotrophin in neurons lacking the cognate TRK (also known as NTRK) receptor[5]). *p75NTR* is more restricted to specific neuronal classes than *DR6*, and its genetic deletion provided only modest protection of sensory axons in the first 36 h after trophic deprivation (Supplementary Fig. 15), as reported previously for sympathetic axons[30]. In sympathetic neurons, p75NTR is thought to mediate competition for NGF: cells with high NGF/TRKA signalling upregulate expression of BDNF, which acts via p75NTR to trigger degeneration of neighbouring neurons with less robust NGF/TRKA signalling[30,31]. This mechanism shares with ours the expression of a prodegenerative ligand(s) by the neurons themselves. However, the DR6 ligand APP is activated by trophic-factor deprivation, whereas p75NTR ligand expression is increased by trophic-factor stimulation[31]. Thus, p75NTR ligands are released by 'strong' neurons to kill 'weak' neurons (a paracrine prodegenerative effect)[31], whereas APP gets activated within weak neurons to accelerate self-destruction

triggered by trophic deprivation or perhaps other insults (an autocrine prodegenerative effect).

Caspase 6 mediates axonal degeneration

The intracellular mechanisms of axonal degeneration and their relation to apoptosis have been unclear. Our results indicate that developmental axonal degeneration does involve an apoptotic pathway, but with a non-classical effector, caspase 6. Epistatis analysis supports a linear activation model from DR6 to BAX to caspase 6, but does not exclude the possibility that active caspase 6 might feedback, for example, to accelerate the process; in this context, it is intriguing that the APP cytoplasmic domain is a caspase 6 substrate[32]. Activation of caspase 6 by trophic deprivation occurs in a punctate pattern in axons, leading to a beads-on-a-string appearance, and sites of punctate caspase 6 activation correspond to sites of microtubule fragmentation. Caspase 6 might trigger microtubule destabilization by cleaving microtubule associated proteins such as TAU (also known as MAPT), a documented target of caspase 6 (refs 33, 34); in a recent proteomic analysis, almost half the identified caspase 6 targets were cytoskeleton-associated[35].

Ligands, receptors for self-destruction

Although p75NTR also binds APP(1–286), DR6 binds with a much higher affinity, and blocking DR6 function largely blocks both APP(1–286) binding to sensory axons and degeneration triggered by APP(1–286). Thus, DR6 seems to be the major functional APP receptor in these neurons, although p75NTR might contribute in other contexts. Conversely, APP may not be the only DR6 ligand: APLP2, which is coexpressed with APP in many neurons[27], may also contribute to degeneration, because an N-terminal fragment is shed in response to trophic deprivation, can bind DR6, and can trigger degeneration when added exogenously (Supplementary Fig. 16). Future studies will define the relative contributions of APP and APLP2 in different neuronal populations.

The finding of similar neuromuscular junction phenotypes in *DR6* and $App^{-/-}$ $Aplp2^{-/-}$ mutants supports a ligand–receptor interaction, and indicates that APP and APLP2 both contribute in this system. The aberrant axonal extensions seen could reflect an impairment of pruning, or, alternatively, a failure of axons to stop; of note, the APP ectodomain has been implicated in neurite growth inhibition[36]. Previous studies have not reported changes in neuronal cell death *in vivo* in *App* mutants, either singly or in combination with *Aplp1* and/or *Aplp2* mutations[37,38]. However, such studies did not examine spinal cord or sensory ganglia, nor involve time-course analysis to evaluate possible delays in degeneration. *In vitro* analysis of cortical neurons from mutants has given divergent results about their basal survival rates and susceptibility to glutamate excitotoxicity[37–39], but their response to trophic deprivation has not been reported.

In recent findings paralleling ours, trophic deprivation was found to trigger BACE cleavage of APP in PC12 cell-derived neurons and primary hippocampal neurons, and degeneration was reduced by *App* knockdown (in PC12 cells) and BACE inhibition[40,41]. The prodegenerative function of APP was, however, attributed to amyloid-β, because antibodies to amyloid-β inhibited degeneration[40,41]. We too observed protection by antibody 4G8, but attribute this to the ability of 4G8 to bind full-length APP and inhibit cleavage, because a different anti-amyloid-β antibody that does not bind native APP inhibited neither shedding nor physiological degeneration, but blocked the toxic action of added amyloid-β. Conversely, the toxic effect of amyloid-β was not blocked by DR6 inhibition. It was also found that a γ-secretase inhibitor, which reduced amyloid-β production after BACE cleavage, inhibited degeneration[40,41]. We too found that γ-secretase inhibitors can partially inhibit degeneration of commissural and sensory axons (Supplementary Fig. 17), but γ-secretase has many substrates, and it is possible that the efficient activation of DR6 signalling requires a distinct γ-secretase-dependent process. Thus, our results argue against the involvement of amyloid-β in initiating DR6-dependent degeneration in the neurons studied here, but this does not exclude its possible involvement in other neurons, or at later times in these neurons to augment the effects of APP–DR6 signalling.

APP–DR6 signalling and neurodegeneration

APP is expressed in adult brain and upregulated in damaged axons[42]. *DR6* is also highly expressed in adult brain (Supplementary Fig. 18). Given our findings, it is reasonable to assume that the APP–death-receptor mechanism might contribute to adult plasticity, or to neurodegeneration after injury or in disease. Interestingly, *DR6* is upregulated in injured neurons[43], raising the question as to whether overexpressed DR6 in neurons can trigger ligand-independent degeneration, as reported for p75NTR[11].

Given the genetic evidence linking APP and its cleavage to Alzheimer's disease, we propose that signalling of APP via DR6 (and possibly p75NTR) may in particular contribute to the initiation or progression of Alzheimer's disease, either alone or in combination with other proposed APP-dependent mechanisms, such as amyloid-β toxicity[21,22] or effects of the APP intracellular domain[44]. Of note, previous studies showed immunoreactivity for the APP N terminus associated with Alzheimer's plaques[45,46], *DR6* maps to chromosome 6p12.2-21.1, near a putative Alzheimer's disease susceptibility locus[47], and sites of *DR6* mRNA expression in adult brain correlate in an intriguing way with known sites of dysfunction in Alzheimer's: very high in hippocampus, high in cortex, but low in striatum (Supplementary Fig. 18), and high in forebrain cholinergic neurons[48], for instance. In addition, activated caspase 6, a downstream DR6 effector, is associated with plaques and tangles in Alzheimer's disease, and with mild cognitive impairment[34,49], consistent with the possible activation of caspase 6 in neuritic processes by the APP–death-receptor mechanism (caspase 6 is also implicated in Huntington's disease[50]). Although these results are compatible with the involvement of APP–DR6 signalling in Alzheimer's, it is less clear how the mechanism fits with genetic evidence implicating altered γ-secretase processing in this disease[19–22]. However, the fact that γ-secretase inhibitors antagonize DR6-dependent degeneration hints at a possible relationship.

Thus, further study is required to determine the full implications of the APP–death-receptor mechanism in development, adult physiology and disease. Nonetheless, our results already tie APP to a new mechanism for neuronal self-destruction in development, and suggest that the APP ectodomain, acting via DR6 and caspase 6, contributes to the pathophysiology of Alzheimer's disease.

METHODS SUMMARY

Antibodies to the following targets were used: procaspase 3 (1:200, Upstate), active capsase 3 (1:200, R&D), procaspase 6 (1:200, Stratagene), active caspase 6 (1:100, BioVision), Tuj1 (1:500, Covance), p75NTR (Chemicon), 2H3 (1:200, DSHB), Islet1/2 (1:100, Santa Cruz Biotech), N-APP (polyclonal, 1:100, Thermo Fisher Scientific; monoclonal 22C11, Calbiochem), DR6 (R&D), NGF (Abcam and Genentech), BDNF (Calbiochem), NT3 (Genentech), amyloid-β (4G8, Covance), the C-terminal cleavage-specific anti-amyloid-β antibody (anti-Aβ(33–42), Sigma), and the C-terminal cleavage site of sAPPβ (Covance). Monoclonal antibodies to human DR6 ectodomain fused with human Fc (A.N., K. Dodge, V. Dixit and M.T.L., manuscript in preparation) were screened for binding to murine DR6 and block of commissural neuron degeneration. Proteins used were: netrin-1 (R&D), NGF (Roche), BDNF and NT3 (Calbiochem), and control IgG (R&D). Transiently expressed murine DR6 ectodomain (amino acids 1–349) fused to human Fc, His-tagged human APP(1–286), and APP(1–286) and APLP2(1–300) fused to human Fc, were affinity-purified from CHO cell supernatants (similar results were obtained using APP(1–286) and APP(1–306), Novus Biologicals). Inhibitors were used against: caspase 3 (Z-DEVD-FMK, Calbiochem), caspase 6 (Z-VEID-FMK, BD Pharmingen), BACE (OM99-2, Calbiochem; BACE inhibitor IV, Calbiochem; AZ29, Genentech), γ-secretase (DAPT, Calbiochem).

See Methods for details of *in situ* hybridization and immunohistochemistry, explant, dissociated, and Campenot chamber cultures, siRNA transfection,

tracing and quantification of retinotectal projections, alkaline-phosphatase-binding assays and pull-down assays.

Full Methods and any associated references are available in the online version of the paper at www.nature.com/nature.

Received 24 May; accepted 31 December 2008.

1. Raff, M. C., Whitmore, A. V. & Finn, J. T. Axonal self-destruction and neurodegeneration. *Science* **296,** 868–871 (2002).
2. Luo, L. & O'Leary, D. D. Axon retraction and degeneration in development and disease. *Annu. Rev. Neurosci.* **28,** 127–156 (2005).
3. Buss, R. R., Sun, W. & Oppenheim, R. W. Adaptive roles of programmed cell death during nervous system development. *Annu. Rev. Neurosci.* **29,** 1–35 (2006).
4. Saxena, S. & Caroni, P. Mechanisms of axon degeneration: from development to disease. *Prog. Neurobiol.* **83,** 174–191 (2007).
5. Haase, G., Pettmann, B., Raoul, C. & Henderson, C. E. Signaling by death receptors in the nervous system. *Curr. Opin. Neurobiol.* **18,** 284–291 (2008).
6. Kuida, K. *et al.* Decreased apoptosis in the brain and premature lethality in CPP32-deficient mice. *Nature* **384,** 368–372 (1996).
7. White, F. A., Keller-Peck, C. R., Knudson, C. M., Korsmeyer, S. J. & Snider, W. D. Widespread elimination of naturally occurring neuronal death in *Bax*-deficient mice. *J. Neurosci.* **18,** 1428–1439 (1998).
8. Finn, J. T. *et al.* Evidence that Wallerian degeneration and localized axon degeneration induced by local neurotrophin deprivation do not involve caspases. *J. Neurosci.* **20,** 1333–1341 (2000).
9. Kuo, C. T., Zhu, S., Younger, S., Jan, L. Y. & Jan, Y. N. Identification of E2/E3 ubiquitinating enzymes and caspase activity regulating *Drosophila* sensory neuron dendrite pruning. *Neuron* **51,** 283–290 (2006).
10. Williams, D. W., Kondo, S., Krzyzanowska, A., Hiromi, Y. & Truman, J. W. Local caspase activity directs engulfment of dendrites during pruning. *Nature Neurosci.* **9,** 1234–1236 (2006).
11. Plachta, N. *et al.* Identification of a lectin causing the degeneration of neuronal processes using engineered embryonic stem cells. *Nature Neurosci.* **10,** 712–719 (2007).
12. Sagot, Y. *et al.* Bcl-2 overexpression prevents motoneuron cell body loss but not axonal degeneration in a mouse model of a neurodegenerative disease. *J. Neurosci.* **15,** 7727–7733 (1995).
13. Watts, R. J., Hoopfer, E. D. & Luo, L. Axon pruning during *Drosophila* metamorphosis: evidence for local degeneration and requirement of the ubiquitin-proteasome system. *Neuron* **38,** 871–885 (2003).
14. Bodmer, J. L., Schneider, P. & Tschopp, J. The molecular architecture of the TNF superfamily. *Trends Biochem. Sci.* **27,** 19–26 (2002).
15. Bossen, C. *et al.* Interactions of tumor necrosis factor (TNF) and TNF receptor family members in the mouse and human. *J. Biol. Chem.* **281,** 13964–13971 (2006).
16. Pan, G. *et al.* Identification and functional characterization of DR6, a novel death domain-containing TNF receptor. *FEBS Lett.* **431,** 351–356 (1998).
17. Zhao, H. *et al.* Impaired c-Jun amino terminal kinase activity and T cell differentiation in death receptor 6-deficient mice. *J. Exp. Med.* **194,** 1441–1448 (2001).
18. Schmidt, C. S. *et al.* Enhanced B cell expansion, survival, and humoral responses by targeting death receptor 6. *J. Exp. Med.* **197,** 51–62 (2003).
19. Walsh, D. M. *et al.* The APP family of proteins: similarities and differences. *Biochem. Soc. Trans.* **35,** 416–420 (2007).
20. Reinhard, C., Hebert, S. S. & De Strooper, B. The amyloid-β precursor protein: integrating structure with biological function. *EMBO J.* **24,** 3996–4006 (2005).
21. Hardy, J. & Selkoe, D. J. The amyloid hypothesis of Alzheimer's disease: progress and problems on the road to therapeutics. *Science* **297,** 353–356 (2002).
22. Haass, C. & Selkoe, D. J. Soluble protein oligomers in neurodegeneration: lessons from the Alzheimer's amyloid β-peptide. *Nature Rev. Mol. Cell Biol.* **8,** 101–112 (2007).
23. Wang, H. & Tessier-Lavigne, M. *En passant* neurotrophic action of an intermediate axonal target in the developing mammalian CNS. *Nature* **401,** 765–769 (1999).
24. Campenot, R. B., Walji, A. H. & Draker, D. D. Effects of sphingosine, staurosporine, and phorbol ester on neurites of rat sympathetic neurons growing in compartmented cultures. *J. Neurosci.* **11,** 1126–1139 (1991).
25. Cole, S. L. & Vassar, R. BACE1 structure and function in health and Alzheimer's disease. *Curr. Alzheimer Res.* **5,** 100–120 (2008).
26. Edwards, P. D. *et al.* Application of fragment-based lead generation to the discovery of novel, cyclic amidine β-secretase inhibitors with nanomolar potency, cellular activity, and high ligand efficiency. *J. Med. Chem.* **50,** 5912–5925 (2007).
27. Slunt, H. H. *et al.* Expression of a ubiquitous, cross-reactive homologue of the mouse β-amyloid precursor protein (APP). *J. Biol. Chem.* **269,** 2637–2644 (1994).
28. Hilbich, C., Monning, U., Grund, C., Masters, C. L. & Beyreuther, K. Amyloid-like properties of peptides flanking the epitope of amyloid precursor protein-specific monoclonal antibody 22C11. *J. Biol. Chem.* **268,** 26571–26577 (1993).
29. Wang, P. *et al.* Defective neuromuscular synapses in mice lacking amyloid precursor protein (APP) and APP-like protein 2. *J. Neurosci.* **25,** 1219–1225 (2005).
30. Singh, K. K. *et al.* Developmental axon pruning mediated by BDNF-p75NTR-dependent axon degeneration. *Nature Neurosci.* **11,** 649–658 (2008).
31. Deppmann, C. D. *et al.* A model for neuronal competition during development. *Science* **320,** 369–373 (2008).
32. LeBlanc, A., Liu, H., Goodyer, C., Bergeron, C. & Hammond, J. Caspase-6 role in apoptosis of human neurons, amyloidogenesis, and Alzheimer's disease. *J. Biol. Chem.* **274,** 23426–23436 (1999).
33. Horowitz, P. M. *et al.* Early N-terminal changes and caspase-6 cleavage of tau in Alzheimer's disease. *J. Neurosci.* **24,** 7895–7902 (2004).
34. Guo, H. *et al.* Active caspase-6 and caspase-6-cleaved tau in neuropil threads, neuritic plaques, and neurofibrillary tangles of Alzheimer's disease. *Am. J. Pathol.* **165,** 523–531 (2004).
35. Klaiman, G., Petzke, T. L., Hammond, J. & Leblanc, A. C. Targets of caspase-6 activity in human neurons and Alzheimer disease. *Mol. Cell. Proteomics* **7,** 1541–1555 (2008).
36. Young-Pearse, T. L., Chen, A. C., Chang, R., Marquez, C. & Selkoe, D. J. Secreted APP regulates the function of full-length APP in neurite outgrowth through interaction with integrin β1. *Neural Develop.* **3,** 15 (2008).
37. Heber, S. *et al.* Mice with combined gene knock-outs reveal essential and partially redundant functions of amyloid precursor protein family members. *J. Neurosci.* **20,** 7951–7963 (2000).
38. Perez, R. G., Zheng, H., Van der Ploeg, L. H. & Koo, E. H. The β-amyloid precursor protein of Alzheimer's disease enhances neuron viability and modulates neuronal polarity. *J. Neurosci.* **17,** 9407–9414 (1997).
39. Han, P. *et al.* Suppression of cyclin-dependent kinase 5 activation by amyloid precursor protein: a novel excitoprotective mechanism involving modulation of Tau phosphorylation. *J. Neurosci.* **25,** 11542–11552 (2005).
40. Matrone, C. *et al.* Activation of the amyloidogenic route by NGF deprivation induces apoptotic death in PC12 cells. *J. Alzheimers Dis.* **13,** 81–96 (2008).
41. Matrone, C., Ciotti, M. T., Mercanti, D., Marolda, R. & Calissano, P. NGF and BDNF signaling control amyloidogenic route and Aβ production in hippocampal neurons. *Proc. Natl Acad. Sci. USA* **105,** 13139–13144 (2008).
42. Medana, I. M. & Esiri, M. M. Axonal damage: a key predictor of outcome in human CNS diseases. *Brain* **126,** 515–530 (2003).
43. Chiang, L. W. *et al.* An orchestrated gene expression component of neuronal programmed cell death revealed by cDNA array analysis. *Proc. Natl Acad. Sci. USA* **98,** 2814–2819 (2001).
44. Muller, T., Meyer, H. E., Egensperger, R. & Marcus, K. The amyloid precursor protein intracellular domain (AICD) as modulator of gene expression, apoptosis, and cytoskeletal dynamics-relevance for Alzheimer's disease. *Prog. Neurobiol.* **85,** 393–406 (2008).
45. Van Gool, D., De Strooper, B., Van Leuven, F. & Dom, R. Amyloid precursor protein accumulation in Lewy body dementia and Alzheimer's disease. *Dementia* **6,** 63–68 (1995).
46. Palmert, M. R. *et al.* Antisera to an amino-terminal peptide detect the amyloid protein precursor of Alzheimer's disease and recognize senile plaques. *Biochem. Biophys. Res. Commun.* **156,** 432–437 (1988).
47. Bertram, L. & Tanzi, R. E. Alzheimer's disease: one disorder, too many genes? *Hum. Mol. Genet.* **13,** R135–R141 (2004).
48. Doyle, J. P. *et al.* Application of a translational profiling approach for the comparative analysis of CNS cell types. *Cell* **135,** 749–762 (2008).
49. Albrecht, S. *et al.* Activation of caspase-6 in aging and mild cognitive impairment. *Am. J. Pathol.* **170,** 1200–1209 (2007).
50. Graham, R. K. *et al.* Cleavage at the caspase-6 site is required for neuronal dysfunction and degeneration due to mutant huntingtin. *Cell* **125,** 1179–1191 (2006).

Supplementary Information is linked to the online version of the paper at www.nature.com/nature.

Acknowledgements We thank R. Axel, C. Bargmann, B. de Strooper, V. Dixit, C. Henderson, J. Lewcock, R. Scheller, R. Vassar, R. Watts, and members of the M.T.-L. laboratory for helpful discussions and suggestions, and critical reading of the manuscript, and A. Bruce for making the diagrams. We thank P. Hass and members of his laboratory (Genentech) for generation and purification of the DR6 ectodomain and APP(1–286), and W.-C. Liang and Y. Wu (Genentech) for binding experiments with purified proteins. Supported by Genentech (A.N. and M.T.-L.) and National Eye Institute grant R01 EY07025 (D.D.M.O.'L.).

Author Contributions A.N. performed most of the experiments, with the exception of the analysis of retinal projections and the experiments listed in the Acknowledgements, and co-wrote the paper. The retinotectal analysis was performed by T.M. and supervised by D.D.M.O.'L. M.T.-L. supervised or co-supervised all experiments, and co-wrote the paper.

Author Information Reprints and permissions information is available at www.nature.com/reprints. The authors declare competing financial interests: details accompany the full-text HTML version of the paper at www.nature.com/nature. Correspondence and requests for materials should be addressed to M.T.-L. (marctl@gene.com).

METHODS

***In situ* hybridization and immunochemistry.** Radioactively labelled ^{35}S *in situ* mRNA hybridization was as described[51], using the mRNA locator kit (Ambion). Radiolabelled mRNA probes to antisense sequences of mouse TNF receptor superfamily member 3′ untranslated regions were generated using the MAXIscript kit (Ambion). Immunochemistry was as described on sections[51] or cultured cells[52]. Surface labelling was done without detergent. Double labelling was performed using Zenon Technology (Invitrogen). Fluorescent caspase reporter assays were as recommended (MP Biologicals). TUNEL assays was as recommended (*in situ* cell death detection kit, Roche).

Quantification of axon degeneration. To measure the percentage of degenerating axon bundles, the number of still visible bundles that showed breakdown was counted.

Quantification on sections. Twenty-micrometre serial cryosections were taken from axially matched cervical (C1–C3) levels of *DR6*$^{-/-}$ embryos and heterozygous littermates. Motor neurons were counted in all sections at E14.5 (large Islet1/2-positive ventral neurons; 4 mutants, 3 controls) or E18 (large H&E-stained ventral neurons; 7 mutants, 5 controls).

Neuronal cultures. E13 rat dorsal spinal cord was dissected after the introduction of plasmids and siRNAs by electroporation[53]; the dorsal explant survival assay was as described[23]. *DR6* siRNA1 and siRNA2 (sense) were 5′-CAAUAGGUCAGGAAGAUGGCU-3′ and 5′-AAUCUGUUGAGUUCAUGCCUU-3′, respectively. The mismatch sequence complementary to siRNA1 was 5′-GGACTCTGTGTACAGTCACCTCCCAGATCTGTTATAG-3′. Mouse sensory and motor neuron explants or dissociated cells were cultured on laminin-coated 35-mm tissue culture dishes in culture medium (Neurobasal medium with B27 supplement) with appropriate trophic factor (sensory: NGF, 50 μg ml^{-1}; motor: BDNF and NT3, 10 μg ml^{-1}). Trophic deprivation was achieved by removing growth factor and adding appropriate antibodies (sensory: anti-NGF, 50 μg ml^{-1}; motor: anti-BDNF and anti-NT3, 50 μg ml^{-1}). The introduction of siRNAs into dissociated sensory neuron cultures was performed as described[54].

Campenot chamber assay. The Campenot chamber assay was carried out as described[24] with minor modifications. In brief, 35-mm tissue culture dishes were coated with poly-D-lysine and laminin and scratched with a pin rake (Tyler Research) to generate tracks, as illustrated in Fig. 2a. A drop of culture medium containing 4 mg ml^{-1} methylcellulose was placed on the scratched substratum. A teflon divider (Tyler Research) was seated on silicone grease and a dab of silicone grease was placed at the mouth of the centre slot. Dissociated sensory neurons from E12.5 mouse DRGs were suspended in methylcellulose-containing medium, loaded into a disposable sterile syringe fitted with a 22-gauge needle, injected into the centre slot under a dissecting microscope, and allowed to settle overnight. The outer perimeter of the dish (the cell body compartment) and the inner axonal compartments were filled with methylcellulose-containing medium. Within 3–5 days *in vitro*, axons begin to emerge into left and right compartments. To trigger local axonal degeneration, NGF-containing medium from axonal compartments was replaced with neurobasal medium containing anti-NGF. Where indicated, anti-DR6.1 or control IgG were added (50 μg ml^{-1} final concentration) at the time of NGF deprivation. Cultures were fixed at different times after deprivation with 4% paraformaldehyde for 30 min at room temperature and processed for TuJ1 immunofluorescence.

Tracing of RGC axons. Injections of DiI into temporal retina and subsequent analyses were performed essentially as previously described[55]. The centre of the termination zone was determined to be the centre of a circumscribed circle. Injection size, termination zone size and the efficiency of axon labelling were not different between wild-type and mutant. The termination zone position was also unchanged (average termination zone centre: 50.3% for controls and 49.8% for mutants ($P > 0.9$), from the medial edge). The retina in mutants appeared morphologically normal, with all retinal layers present in similar proportions to wild-type.

For quantification, the presence of axons was determined in 100-μm vibratome sections and transposed onto the superior colliculus. Sections were photographed and axon presence was recorded in 100-μm segments from the anterior border. Using landmarks such as the termination zone, unique arbors, or the edge of the superior colliculus, these data were transposed from photos of sections to photos of the wholemount superior colliculuses in dorsal view, resulting in a grid of 100-μm squares covering each superior colliculus. The termination zones and grids were aligned for the analyses. All analyses were performed blinded to genotype.

Alkaline phosphatase binding assays. Alkaline phosphatase fused to the DR6 ectodomain (DR6–AP) and to APP(1–286) (APP–AP) were transiently expressed in COS-1 cells. Medium was changed after 12 h to OPTI-MEM (Invitrogen), and conditioned medium was collected 36 h later and filtered.

The DR6–AP blot assay on conditioned medium was performed as described[56]. In brief, conditioned medium derived from sensory axons maintained in Campenot chambers or ventral spinal cord explants in explant culture (with or without trophic deprivation) was concentrated tenfold using centriprep centrifugal filters (Millipore), resolved in 4–20% gels under non-reducing conditions, and blotted with DR6–AP in alkaline phosphatase binding buffer.

For *in situ* sensory axon binding assays, wild-type or *Bax*$^{-/-}$ sensory explants were cultured, deprived of NGF for 12 h (with or without BAX inhibitor, as indicated), then washed twice with the alkaline phosphatase binding buffer (HBSS, Gibco, with 0.2% BSA, 0.1% NaN_3, 5 mM $CaCl_2$, 1 mM $MgCl_2$, 20 mM HEPES, pH 7.0). The alkaline phosphatase binding assay was carried out by making a 1:1 mixture of binding buffer and conditioned medium containing DR6–AP, APP–AP, or control alkaline phosphatase, applied to DRG explants in 8-well culture slides and incubated for 90 min at room temperature. Explants were rinsed five times with binding buffer, fixed with formaldehyde (3.7% in PBS) for 12 min at room temperature, and rinsed three times with HBS (20 mM HEPES, pH 7.0, 150 mM NaCl). Endogenous alkaline phosphatase activity was blocked by heat inactivation at 65 °C in HBS for 30 min. After rinsing three times in alkaline phosphatase reaction buffer (100 mM Tris, pH 9.5, 100 mM NaCl, 50 mM $MgCl_2$), bound alkaline phosphatase fusion was visualized by developing colour stain in alkaline phosphatase reaction buffer with 1/50 (by volume) of NBT/BCIP stock solution (Roche) overnight at room temperature.

The *in situ* binding of DR6–AP to COS cells transiently expressing APP695 was performed in the same way, but with heparin (2–10 μg ml^{-1}) added to reduce nonspecific binding. DR6–AP did not bind to controls (p75NTR or DR6 expressed in COS-1 cells) under these conditions. For quantitative analysis, the amount of DR6–AP protein in medium was quantified as described[57]. In brief, 100 μl of 2× alkaline phosphatase buffer (prepared by adding 100 mg para-nitrophenyl phosphate (Sigma) and 15 ml of 1 M $MgCl_2$ to 15 ml 2 M diethanolamine, pH 9.8) was mixed with conditioned medium containing DR6–AP or control alkaline phosphatase. The reaction was developed over 5–15 min, with the absorbance being in the linear range (0.1–1). The volume of reaction was adjusted by adding 800 μl of distilled water, and absorbance was measured at 405 nm. Concentration in nM was calculated according to the formula (for 100 ml): $C\,(\mathrm{nM}) = A \times 100 \times (60/\text{developing time})/30$. Saturation binding analysis was performed as described[57]. Prizm 4 software (GraphPad) was used to generate saturation binding curves and to determine half-maximal saturation value.

APP pull-down assays. Soluble ectodomains of TNF receptor superfamily members fused to human Fc were expressed in CHO cells and affinity purified. They were incubated at 5 μg ml^{-1} in binding buffer (HBSS, with 0.2% BSA, 0.1% NaN_3, 5 mM $CaCl_2$, 1 mM $MgCl_2$, 20 mM HEPES, pH 7.0) with 1 μg ml^{-1} of His-tagged APP(1–286) and protein A/G beads (Santa Cruz Bio) at 4 °C overnight. Beads were washed five times with binding buffer. Bound complexes were eluted from beads with SDS loading buffer, resolved in 4–20% SDS PAGE gels, and blotted for APP (with anti-NAPP(poly)) and for TNF receptor family members (with anti-human Fc).

Mice. The following mutant mice were used: *DR6* knockout[17] (gift from V. Dixit), *Bax* knockout[58] (gift from S. Korsmeyer) and *p75NTR* knockout[59] (Jackson laboratory).

51. Sabatier, C. *et al.* The divergent Robo family protein rig-1/Robo3 is a negative regulator of slit responsiveness required for midline crossing by commissural axons. *Cell* **117**, 157–169 (2004).
52. Atwal, J. K. *et al.* PirB is a functional receptor for myelin inhibitors of axonal regeneration. *Science* **322**, 967–970 (2008).
53. Chen, Z. *et al.* Alternative splicing of the Robo3 axon guidance Receptor governs the midline switch. *Neuron* **58**, 325–332 (2008).
54. Higuchi, H., Yamashita, T., Yoshikawa, H. & Tohyama, M. Functional inhibition of the p75 receptor using a small interfering RNA. *Biochem. Biophys. Res. Commun.* **301**, 804–809 (2003).
55. McLaughlin, T., Torborg, C. L., Feller, M. B. & O'Leary, D. D. Retinotopic map refinement requires spontaneous retinal waves during a brief critical period of development. *Neuron* **40**, 1147–1160 (2003).
56. Pettmann, B. *et al.* Biological activities of nerve growth factor bound to nitrocellulose paper by western blotting. *J. Neurosci.* **8**, 3624–3632 (1988).
57. Okada, A. *et al.* Boc is a receptor for sonic hedgehog in the guidance of commissural axons. *Nature* **444**, 369–373 (2006).
58. Knudson, C. M. *et al.* Bax-deficient mice with lymphoid hyperplasia and male germ cell death. *Science* **270**, 96–99 (1995).
59. Lee, K. F. *et al.* Targeted mutation of the gene encoding the low affinity NGF receptor p75 leads to deficits in the peripheral sensory nervous system. *Cell* **69**, 737–749 (1992).